Author/s:
Wu, W;Westra, S;Leonard, M

Title:
A basis function approach for exploring the seasonal and spatial features of storm surge events

Date:
2017-07-28

Citation:
Wu, W., Westra, S. & Leonard, M. (2017). A basis function approach for exploring the seasonal and spatial features of storm surge events. Geophysical Research Letters, 44 (14), pp.7356-7365. https://doi.org/10.1002/2017GL074357.

Wu Wenyan (Orcid ID: 0000-0003-3907-1570)
Westra Seth (Orcid ID: 0000-0003-4023-6061)

A basis function approach for exploring the seasonal and spatial features of storm surge events

Wenyan Wu[1], Seth Westra[1], and Michael Leonard[1]

[1]School of Civil, Environmental and Mining Engineering, University of Adelaide.

Corresponding author: Wenyan Wu, wenyan.wu@adelaide.edu.au

Key Points:

- Basis functions are used to simulate storm surge events, enabling an analysis of the temporal progression of surge events.
- Seasonal and spatial variability in storm surge attributes provides more insights for flood risk in coastal and estuarine regions.
- The relationship between peak and decay rate of storm surge during dominant seasons has significant implications on flood risk.

This is the author manuscript accepted for publication and has undergone full peer review but has not been through the copyediting, typesetting, pagination and proofreading process, which may lead to differences between this version and the Version of Record. Please cite this article as doi: 10.1002/2017GL074357

Abstract

Storm surge is a significant contributor to flooding in coastal and estuarine regions. To represent the statistical characteristics of storm surge over a climatologically diverse region, we propose the use of basis functions that capture the temporal progression of individual storm surge events. This extends statistical analyses of surge from considering only the peak to a more multi-faceted approach that also includes decay rate and duration. Our results show that there is seasonal variation in storm surge along the Australian coastline. During the dominant storm surge seasons, the peak and duration of storm surge events tend to increase simultaneously at a number of locations, with implications for flood damage assessments and evacuation planning. By combining the dynamic and statistical features of storm surge, it is possible to better understand the factors that can lead to flood risk along the coastline, including estuarine areas that are also affected by fluvial floods.

1 Introduction

Storm surge caused by low pressure and wind stress acting on ocean's surface can be a large component of extreme ocean water levels [*Serafin et al.*, 2017], potentially placing millions of people and trillions of dollars of assets at risk globally [*Hanson et al.*, 2011]. To prepare for and mitigate such damaging events, it is critical to understand the unique characteristics of surges, including how they vary in time, their seasonal variability and how the features of surges vary along a coastline. To this end, risk assessment methods are a critical tool in describing implications of surge on flood potential, and are informed by an understanding of both the dynamic characteristics of surge (including the peak, duration and temporal evolution of surge events) that collectively determine the flood damage, and the statistical features of surge that help describe event probability. However, in many cases the dynamic and statistical attributes of surge have been explored in isolation, posing difficulties for developing a unified understanding of the factors that contribute to flood risk.

The dynamic aspects of surge have typically been assessed through hydrodynamic modelling studies, with applications in recreating historical surge events [*Bilskie et al.*, 2016a; *Yin et al.*, 2016], understanding causal mechanisms [*Haigh et al.*, 2014b; *Kodaira et al.*, 2016; *Lapetina and Sheng*, 2015] and estimating the implications of future changes to those events [*Bilskie et al.*, 2014; *Bilskie et al.*, 2016b; *Izuru et al.*, 2015; *Oey and Chou*, 2016]. An advantage of these studies is that by solving the governing equations of fluid motion, they preserve faithfulness to the underlying physics, and often allow realistic depiction of real-world storm surge events, including inundation across normally dry coastal areas. However, such methods are often limited by data requirements [*Madsen et al.*, 2015], including lack of data availability and/or insufficient spatial or temporal resolution [*Colberg and McInnes*, 2012]. Additionally, hydrodynamic models are computationally expensive, which can limit their ability to simulate large ensembles of events [*Nuswantoro et al.*, 2016] as often required for risk calculations [*Ball et al.*, 2016].

In contrast, studies of the statistical aspects of storm surge have focused on describing surge peaks, usually with a view to understanding the probability of rare but potentially catastrophic surge events. Typical applications include the use of statistical models to estimate maximum surge caused by tropical storms [*Irish et al.*, 2011] and surge probabilities [*Irish et al.*, 2009; *Irish et al.*, 2011] and to understand characteristics of extreme surge [*Coles and Tawn*, 2005a; b], long term variation in storm surge [*Oh et al.*, 2016] and potential impact of climate change [*Balaguru et al.*, 2016]. In addition, a number of statistical models exist that consider the relationship between surge and other processes that contribute to flooding in coastal and estuarine regions, such as waves [*Wolf and Flather*, 2005], winds [*Pirazzoli*, 2000], and tides [*Feng et al.*, 2015; *Pugh*, 1982; *Williams et al.*, 2016], as well as other drivers of estuarine flood hazard such as coastal rainfall and fluvial floods [*Zheng et al.*, 2015]. Variously, these papers emphasize the variation in surge with location, season and climate, and highlight the importance of linking meteorological and hydrodynamic processes with methods of estimating extreme surge [*Coles and Tawn*, 2005b]. However, the focus on single measures of surge magnitude (e.g. peak surge or skew surge) can lead to a loss of dynamic information of storm surge evolution.

To address limitations of the above statistical approaches while maintaining key features of dynamic evolution of storm surge events, this study proposes a novel basis function approach that captures the time-varying features of storm surge including peak, duration and decay rate. This information is then used to explore the seasonal and spatial variability of storm surge along the Australian coastline, as well as how the dynamic features of surge change as the peaks become more extreme. This information provides a critical first step in better understanding the processes that lead to extreme surge, and incorporating the temporal progression of surge into statistical analysis of coastal and estuarine flood hazard and risk.

To implement the basis function approach, two separate basis functions were compared and evaluated, the first based on linear growth and decay curves, and the second assuming exponential growth and decay of storm surge (Section 2.2). Both basis functions were evaluated using storm surge data from 15 tide gauges across Australia (Section 2.4). The basis functions were then used to investigate the seasonal and spatial variability of the attributes of storm surge events (Section 3.1) and the seasonal relationship between these attributes (Section 3.2). In addition, the evolution of storm surge events and how it varies seasonally and spatially was also investigated (Section 3.3). Differences in the dynamics and magnitude of surge events with location and season indicate challenging key features that should be incorporated into methods for estimating flood risk in coastal and estuarine regions.

2 Data and Methods

2.1 Data Selection

Hourly storm surge data were obtained from 15 high-quality tide gauges located in climatologically different regions along the Australian coastline (Figure S1 in supporting material). These gauges are monitored as part of the Australian Baseline Sea Level Monitoring Project, which was designed to identify long term sea level changes around Australia (http://www.bom.gov.au/oceanography/projects/abslmp/abslmp.shtml, hourly data openly accessible). The records are from the early 1990s to December 2015, except for Port Stanvac, where the record ends in 2010.

2.2 Overview of Basis Functions

To represent the dynamic features of individual storm surge events, the following two basis functions were used. The exponential function for simulating storm surge events is expressed as:

$$y = \begin{cases} \alpha \times \exp(\beta x), & x \leq 0 \\ \alpha \times \exp(-\beta x), & x > 0 \end{cases} \qquad \text{Eq.(1)}$$

where α represents the peak of the surge event in meters, and β represents the decay rate of the surge event (Figure S2a in the supporting material); i.e. how quickly/slowly the storm surge will reach its peak and reduce back to zero. A large (small) value of β represents a more peaked (flatter) surge event that quickly (slowly) recedes to zero from the peak.

The second basis function is triangular, which can be expressed as:

$$y = \begin{cases} \frac{a}{b}x + a, & x \, \epsilon [-b, 0) \\ -\frac{a}{b}x + a, & x \, \epsilon [0, b] \end{cases} \qquad \text{Eq.(2)}$$

where a represents the peak of the surge event in meters, and b is the time (in hours) when the surge value is reduced to zero from the event peak, so that b is equal to half of the duration of the event (Figure S2b). Both basis functions assume a single peak within one storm surge event with symmetric rising and falling limbs. These assumptions are a tradeoff between computational efficiency and simplicity.

2.3 Use of Basis Functions to Identify Historical Storm Surge Events

The historical storm surge record was defined as the non-tidal residual time series (i.e. the difference between observed water level and modelled astronomical tide, where the modelled astronomical tide was estimated through a harmonic analysis). To identify the peaks of storm surge events, a minimum threshold of the 99th percentile of hourly storm surge was selected for the following reasons:

1) This threshold is equivalent to a 4.2 day return period of hourly water levels, which guarantees that both extreme and moderate surge events are included in deriving the basis functions. This can be important for some applications, as floods are not only caused by extreme surge events, but also by the coincidence of high astronomical tides and/or fluvial floods with moderate surge events [*Sabatino et al.*, 2016].

2) This threshold avoids selecting surge events with a peak value close to the typical errors of harmonic analysis, which can have root-mean-square values ranging from 0.1 m to 0.29 m for regions with low and high tidal ranges respectively [*Williams et al.*, 2016].

The final threshold values for the 15 tide gauges around Australia range from 0.23 m in the south east to 0.62 m on the south coast (Figure S1 in the supporting material). The proposed basis functions are then used to identify storm surge events using the following approach. First, the highest surge value from the entire surge time series is identified at each tide gauge. A basis function (either the exponential or the triangular basis function) is then fitted to the corresponding surge event, and this fitted basis function is subtracted from the time series to create a new "residual" time series with that event removed. This process repeats by finding the highest surge value in the re-calculated residual series and fitting the basis function at that event, and again subtracting the fitted basis function from the series. The entire process is repeated until all values in the residual time series are below the threshold. As a result of this fitting process, each surge event is characterized by the calendar date and time of the peak, and the parameter set of the basis function used (e.g. α and β for the exponential basis function and a and b for the triangular basis function). The outcome of this process led to between 100 and 300 storm surge events being identified at each location, with the specific number of events depending on the location and basis function used. This is equivalent to between four to 12 events per year (based on 25 years' data). The plot of the top 50 identified historical surge events over a 48-hour period for the 15 tide gauges is presented in Figure S3 in the supporting material.

2.4 Basis Function Evaluation and Comparison

A quantile approach was used to examine how well the basis functions preserved the characteristics of observed surge data, with confidence intervals developed using a bootstrap with replacement approach. First, a quantile plot of the time series data of observed surge events was produced. Then 1000 samples were drawn randomly with replacements from the surge events simulated using the fitted basis functions, in order to construct 95% confidence intervals of the observed data. The quantile plots of the observed surge data, as well as the 95% confidence intervals generated using bootstrap resampling with both basis functions, are presented in Figure S4 in the supporting material. It shows that the observed surge data falls within the 95% confidence intervals generated using both basis functions for all 15 locations.

The quantile-based analysis focused on the selected surge events, and therefore includes a combination of both moderate and extreme surge events. To compare the two basis functions in terms of their efficacy in reproducing more extreme surge data above high thresholds, a bias and variability tradeoff concept was used [*Wu et al.*, 2013]. This analysis was based on the 99.9th percentile hourly threshold, which is equivalent to a return period of approximately one month (i.e. 720 hours).

The bias and variability of the two basis functions generated for the 15 tide gauges are presented in Figure S5 of the supporting material. The results show that both basis functions are slightly positively biased, which indicates that both basis functions tend to over-estimate the number of surge data points above the 99.9th percentile threshold. However, the overall bias-variability performance is more dependent on the location rather than the basis function used. For example, relatively high bias and variability were observed for both Darwin and Rosslyn Bay regardless of the basis function used. Additionally, for the majority of the locations (except for Broome and Darwin), the exponential basis function outperforms the triangular basis function in terms of both bias and variability. This indicates that the exponential basis function on average provides a better representation of the storm surge events.

3 Results

All the results are based on the historical surge events extracted using basis functions at each of the 15 locations. Section 3.1 explores the seasonality and spatial variability of the historical surge events by representing the proportion of all events occurring in each season and for different magnitude classes at each of the 15 locations. To explore the relationship between event magnitude (represented by the α parameter of the exponential function) and decay rate (represented by the β parameter of the exponential function), the correlation between the fitted basis function parameters is assessed in Section 3.2. The mean effect of this relationship is then illustrated in Section 3.3 by fitting a curve to basis function parameters, and plotting how surge events simulated using the basis functions along the fitted curve are changing with increasing magnitude across different locations and seasons.

3.1 Seasonal and Spatial Variability of Storm Surge Events

The analysis first explores the seasonal and spatial variability of the delineated storm surge events at each of the 15 tide gauges (i.e. the storm surge events identified using basis functions above the threshold provided in Figure S1). The results are presented in Figure 1, and illustrate large-scale features of variability geographically along the Australian coastline, and also as a function of surge magnitude. In particular, the northern third of the continent experiences more storm surge events in summer (December, January and February) and autumn (March, April and May) compared to winter (June, July and August) and spring (September, October and November) (Figure 1a). Furthermore, the dominance of summer and autumn becomes more pronounced as the magnitude of the events increases (Figure 1b). In contrast with northern Australia, the southern parts of the Australian coastline experience more storm surge events during spring and winter, with this seasonal pattern being evident for all events (Figure 1a) but again most pronounced for the larger events (Figure 1b).

To test if the findings in Figure 1 are statistically significant, bootstrap-based hypothesis tests were used to estimate the significance levels of seasonal variability in the attributes of storm surge events, including peak and half-life (i.e. the time required for a surge event to reach 50% of its maximum magnitude from the peak). The null hypothesis is that there is no seasonal variation in the peak and half-life of storm surge events. If the mean peak or half-life calculated from observed data is outside the 95% confidence interval generated from bootstrap resampling of storm surge events, the null hypothesis is rejected. The results of the hypothesis tests for storm surge event peaks and half-life are presented in Figures 2(a) and 2(b), respectively. As can be seen from Figure 2(a), the magnitude of storm surge events at Broome, Darwin and Groote Eylandt (in the north of Australia) are significantly lower in spring and winter compared to the rest of the year. In contrast, the magnitude of storm surge events at Thevenard, Portland, Stony Point and Burnie (in the south of Australia) are significantly lower in summer compared to the rest of the year.

In contrast to storm surge event peak, seasonal variation in event half-life is less significant at the majority of the locations (Figure 2b), with the exception of Groote Eylandt near the Gulf of Carpentaria in the north and Hillarys near Perth in south west Australia. At Groote Eylandt, the observed mean half-life values fall outside the 95% confidence intervals in both spring and winter, indicating significantly reduced surge durations in the cooler months of the year. At Perth, the observed mean half-life value in summer is above the 97.5th percentile level, indicating significantly longer surge events in this season. Similar results on seasonality of storm surge can be found for events simulated using the triangular basis function, which are presented in Figure S6 of the supporting material.

3.2 Seasonal Relationship between Storm Surge Event Attributes

To explore the temporal characteristics of storm surge events, as well as their seasonal and spatial variability, the relationship between storm surge event attributes was investigated in terms of the basis function parameters (i.e. peak represented by α of the exponential basis function, decay rate represented by β of the exponential basis function, and duration represented by b of the triangular basis function). The rank-based Kendall's τ [1938] was used to examine the correlation between the peak and decay rate, and between the peak and duration, as it is less sensitive to outliers and skewed distributions than Pearson's correlation, and does not rely on the assumption of linearity [*Williams et al.*, 2016]. The null hypothesis is that the two variables are completely independent. The null hypothesis test results are summarized in Tables S1 and S2 in the supporting material. Values highlighted in bold italics indicate statistical significance with $p < 0.05$.

The results for the exponential basis function (Table S1) show that storm surge event peak and decay rate are generally negatively correlated. Considering the annual data, 14 out of the 15 tide gauges exhibited negative correlations, although only five were statistically significant and the typical correlation value is around -0.2 indicating a weak relationship. Negative correlations for the exponential basis function parameters indicate that larger surges exhibit slower growth rates. Considering the seasonal results, four locations in the south of Australia (i.e. Hillarys, Port Stanvac, Lorne and Burnie) exhibit statistically significant relationships in winter, whereas for Darwin in the north of Australia, the relationship is statistically significant in summer and autumn. Common to each of these locations is that the strongest statistical relationships occur during the dominant storm surge season.

The results for the triangular basis function (Table S2) show a statistically significant correlation between peak and duration at nine out of the 15 sites, with the positive correlation between the parameters of this basis function again indicating that larger surges exhibit slower growth rates (i.e. longer durations). For seasonal analysis, the relationship is also significant in winter at four sites in the south of Australia, and in summer and autumn at Darwin in the north. The scatter plots of the attributes of all the selected surge events at different times of the year, as well as the associated Kendall τ and p values for the 15 tide gauges, are presented in Figures S7 to S16 in the supporting material.

3.3 Temporal Evolution of Storm Surge Events

To illustrate the implications of the above findings on how storm surge events evolve during different times of the year around Australia, a smooth curve is fitted to the relationship between the peak and decay rate at three selected locations (Darwin, Hillarys and Lorne), which are representative of the north, south west and south east of Australia. The exponential basis function is then used to simulate eight storm surge events with different peaks selected from the fitted curve. The observed fitted relationships between the storm surge peak and the decay rate are presented in the left-hand side panels, and illustrations of the change in growth rates with increasing peak surge using these fitted values are presented in the right-hand side panels.

As shown in Figure 3 (left panels), at Darwin in summer and Hillarys and Lorne in winter, the decay rate reduces exponentially with the peak of surge events, which results in significantly increased duration of the larger surge events. In contrast, during the non-dominant storm surge seasons (i.e. winter at Darwin and summer at Hillarys and Lorne), there is no significant correlation between the peak and decay rate of surge events. For these situations, the decay rate tends to change little with the peak of surge events, which results in similar durations for surge events with different peaks. This phenomenon is most evident at Darwin, where surge events are almost homogeneous in winter and much smaller compared to summer events in terms of both magnitude and duration.

4 Discussion

Storm surge is an important contributor to flooding in coastal and estuarine regions, affecting not only the magnitude, but also the timing and duration of elevated water levels. A significant challenge accompanying the estimation of flood risk in these regions is that methods must be able to estimate the statistical features of surge that will influence the probability of flood events, as well as the dynamic characteristics of surge (including the peak, duration and temporal evolution) that collectively determine the flood damage and the potential for coincidence with other flood causative mechanisms such as fluvial processes in estuarine regions.

In this study, a novel basis function based approach is proposed to simulate time series of storm surge events for 15 tide gauges around Australia. Two simple two-parameter basis functions assuming a single peak and symmetric rising and falling limbs were used. These assumptions are made considering tradeoff between computational efficiency and simplicity. Other features of surge, such as multiple peaks and asymmetric rising and falling limbs, could in principle be simulated using more complex basis functions, but at the expense of requiring more parameters. The choice of two-parameter basis functions was made in order to capture the main features of storm surge events - i.e. the surge peak and decay - as demonstrated by Figure S3. This simple structure enables efficient statistical analysis of large ensembles of events. The surge event time series simulated using basis functions can also capture the time-varying features of storm surge including peak, duration and decay rate. This dynamic information is then used to explore the seasonal and spatial variability of storm surge along the Australian coastline.

Consistent with expectations, it is evident that summer and autumn are the dominant seasons for storm surge in the north of Australia. For these regions, storm surge events in summer and autumn are more likely to be associated with tropical cyclones or tropical lows, which are frequent in this time of the year and can cause extremely high surge [*Haigh et al.*, 2014b]. In addition, the north of Australia (e.g. Darwin and Gulf Carpentaria) often experiences bursts of northwest monsoon winds in summer, which increases the frequency and magnitude of summer storm surge events [*Haigh et al.*, 2014a]. In contrast to the northern Australia results, spring and winter are the dominant storm surge seasons in the south of Australia. In these regions, there are frequent east-travelling cold fronts associated with low pressure systems in early spring and winter, which bring both onshore winds and heavy rainfall [*McInnes et al.*, 2012], with the wind stress often causing large storm surge events in these regions [*McInnes et al.*, 2009]. Finally, along the east coast of Australia including southern Queensland, New South Wales and eastern Victoria (e.g. Rosslyn Bay, Port Kembla to Portland), the increased frequency and magnitude of storm surge events in spring and winter is mainly associated with east coast lows. Driven by the temperature gradient between the Tasman Sea air and cold air in the high levels of the atmosphere, east coast lows can occur at any time of the year, although most of them occur in the cooler months (i.e. between April and September) [*McInnes and Hubbert*, 2001].

In order to understand the dynamic features of surge change as the peaks become more extreme, we examined the relationships between the peak and decay rate of surge events during different times of the year and how they impact the evolution of storm surge events. The results show that during the dominant storm surge seasons (summer in the north and winter in the south of Australia), there is a weak correlation between the peak and decay rate of storm surge. This correlation results in simultaneous increase in the peak and duration of storm surge events during dominant seasons, which has substantial implications to flood risk estimation and mitigation. When large storm surge events occur in summer in the north and in winter in the south of Australia, not only will they result in increased inundation extent, they will also tend to last longer, leading to potential increases in flood damage and disruption. The increase in duration of storm surge events also increases the probability that the surge event coincides with other extreme conditions, such as a high tide and the peak discharge from an upstream catchment, which leads to a compounding effect on flood. However, it should be cautioned that even for instances where the relationships between surge magnitude and decay are statistically significant, the correlation coefficients are low, indicating significant unexplained variability. Therefore, for flood risk estimation applications, it is important to account for the full variability (e.g. using re-sampling approaches or multivariate statistical distributions) rather than focusing only on the main effect illustrated in Figure 3.

5 Conclusions

The basis function approach provides a unified methodology of evaluating the dynamic features of storm surge events within a statistical analysis. This is useful in extending statistical analysis of storm surge from considering only the peak to including decay and duration information, and can be used to simulate inundation across normally dry coastal areas during surge events, which is currently difficult to produce with statistical approaches. Furthermore, with increased emphasis being focused on understanding "compound events" (i.e. events for which multiple extremes can occur simultaneously or in close succession; see Leonard et al. [2014] and IPCC [2012]), such as the coincidence of astronomical tides, storm surges and fluvial floods in estuarine catchments [*Zheng et al.*, 2015], it is becoming increasingly critical to capture the timing and duration of individual flood drivers. The basis function approach enables new stochastic (e.g. Monte Carlo) approaches for joint probability analysis of flood risks considering these different flood drivers, thereby opening up new avenues not only for understanding the physical nature storm surge events, but also more rigorous joint probability based flood risk estimation approaches that blend the complex dynamic and statistical features that characterize storm surge behavior.

Acknowledgments

We would like to thank Australian Research Council and Western Australian Water Corporation for funding under Linkage Project LP150100359. We thank the Bureau of Meteorology (http://www.bom.gov.au/) for providing the data used in this study.

References

Balaguru, K., D. R. Judi, and L. R. Leung (2016), Future hurricane storm surge risk for the U.S. gulf and Florida coasts based on projections of thermodynamic potential intensity, *Climatic Change*, *138*(1), 99-110.

Ball, J., M. Babister, R. Nathan, W. Weeks, E. Weinmann, M. Retallick, and I. Testoni (Eds.) (2016), *Australian Rainfall and Runoff: A Guide to Flood Estimation*, Commonwealth of Australia (Geoscience Australia), Canbarra, ACT, Australia.

Bilskie, M. V., S. C. Hagen, S. C. Medeiros, and D. L. Passeri (2014), Dynamics of sea level rise and coastal flooding on a changing landscape, *Geophysical Research Letters*, *41*(3), 927-934.

Bilskie, M. V., S. C. Hagen, S. C. Medeiros, A. T. Cox, M. Salisbury, and D. Coggin (2016a), Data and numerical analysis of astronomic tides, wind-waves, and hurricane storm surge along the northern Gulf of Mexico, *Journal of Geophysical Research: Oceans*, *121*(5), 3625-3658.
Bilskie, M. V., S. C. Hagen, K. Alizad, S. C. Medeiros, D. L. Passeri, H. F. Needham, and A. Cox (2016b), Dynamic simulation and numerical analysis of hurricane storm surge under sea level rise with geomorphologic changes along the northern Gulf of Mexico, *Earth's Future*, *4*(5), 177-193.
Colberg, F., and K. L. McInnes (2012), The impact of future changes in weather patterns on extreme sea levels over southern Australia, *Journal of Geophysical Research: Oceans*, *117*(C8).
Coles, S., and J. Tawn (2005a), Seasonal effects of extreme surges, *Stochastic Environmental Research and Risk Assessment*, *19*(6), 417-427.
Coles, S., and J. Tawn (2005b), Bayesian modelling of extreme surges on the UK east coast, *Philosophical Transactions of the Royal Society A: Mathematical, Physical and Engineering Sciences*, *363*(1831), 1387.
Feng, J., H. von Storch, W. Jiang, and R. Weisse (2015), Assessing changes in extreme sea levels along the coast of China, *Journal of Geophysical Research: Oceans*, *120*(12), 8039-8051.
Haigh, I. D., E. M. S. Wijeratne, L. R. MacPherson, C. B. Pattiaratchi, M. S. Mason, R. P. Crompton, and S. George (2014a), Estimating present day extreme water level exceedance probabilities around the coastline of Australia: tides, extra-tropical storm surges and mean sea level, *Climate Dynamics*, *42*(1), 121-138.
Haigh, I. D., L. R. MacPherson, M. S. Mason, E. M. S. Wijeratne, C. B. Pattiaratchi, R. P. Crompton, and S. George (2014b), Estimating present day extreme water level exceedance probabilities around the coastline of Australia: tropical cyclone-induced storm surges, *Climate Dynamics*, *42*(1), 139-157.
Hanson, S., R. Nicholls, N. Ranger, S. Hallegatte, J. Corfee-Morlot, C. Herweijer, and J. Chateau (2011), A global ranking of port cities with high exposure to climate extremes, *Climatic Change*, *104*(1), 89-111.
IPCC (2012), Managing the Risks of Extreme Events and Disasters to Advance Climate Change Adaptation. A Special Report of Working Groups I and II of the Intergovernmental Panel on Climate Change. *Rep.*, 582 pp. pp, Intergovernmental Panel on Climate Change NY, USA.
Irish, J. L., D. T. Resio, and M. A. Cialone (2009), A surge response function approach to coastal hazard assessment. Part 2: Quantification of spatial attributes of response functions, *Natural Hazards*, *51*(1), 183-205.
Irish, J. L., Y. K. Song, and K.-A. Chang (2011), Probabilistic hurricane surge forecasting using parameterized surge response functions, *Geophysical Research Letters*, *38*(3), n/a-n/a.
Izuru, T., H. Kenshi, S. Hidetaka, S. Hideo, M. Nobuhito, S. Yoko, and T. Tetsuya (2015), Climate change effects on the worst-case storm surge: a case study of Typhoon Haiyan, *Environmental Research Letters*, *10*(6), 064011.
Kahle, D., and H. Wickham (2013), ggmap: Spatial Visualization with ggplot2., *The R Journal*, *5*(1), 144-161.

Kendall, M. G. (1938), A New Measure of Rank Correlation, *Biometrika*, *30*(1/2), 81-93.
Kodaira, T., K. R. Thompson, and N. B. Bernier (2016), The effect of density stratification on the prediction of global storm surges, *Ocean Dynamics*, *66*(12), 1733-1743.
Lapetina, A., and Y. P. Sheng (2015), Simulating complex storm surge dynamics: Three-dimensionality, vegetation effect, and onshore sediment transport, *Journal of Geophysical Research: Oceans*, *120*(11), 7363-7380.
Leonard, M., S. Westra, A. Phatak, M. Lambert, B. van den Hurk, K. McInnes, J. Risbey, S. Schuster, D. Jakob, and M. Stafford-Smith (2014), A compound event framework for understanding extreme impacts, *Wiley Interdisciplinary Reviews: Climate Change*, *5*(1), 113-128.
Madsen, K. S., J. L. Høyer, W. Fu, and C. Donlon (2015), Blending of satellite and tide gauge sea level observations and its assimilation in a storm surge model of the North Sea and Baltic Sea, *Journal of Geophysical Research: Oceans*, *120*(9), 6405-6418.
McInnes, K. L., and G. D. Hubbert (2001), The impact of eastern Australian cut-off lows on coastal sea levels, *Meteorological Applications*, *8*(2), 229-243.
McInnes, K. L., I. Macadam, G. D. Hubbert, and J. G. O’Grady (2009), A modelling approach for estimating the frequency of sea level extremes and the impact of climate change in southeast Australia, *Natural Hazards*, *51*(1), 115-137.
McInnes, K. L., et al. (2012), Climate Futures for Tasmania: extreme tide and sea-level events*Rep.*, Antarctic Climate and Ecosystems Cooperative Research Centr, Hobart, Tasmani.
Nuswantoro, R., F. Diermanse, and F. Molkenthin (2016), Probabilistic flood hazard maps for Jakarta derived from a stochastic rain-storm generator, *Journal of Flood Risk Management*, *9*(2), 105-124.
Oey, L.-Y., and S. Chou (2016), Evidence of rising and poleward shift of storm surge in western North Pacific in recent decades, *Journal of Geophysical Research: Oceans*, *121*(7), 5181-5192.
Oh, S. M., I.-J. Moon, and S. J. Kwon (2016), Increasing the highest storm surge in Busan harbor, *Journal of Coastal Research*, *75*(sp1), 760-764.
Pirazzoli, P. A. (2000), Surges, atmospheric pressure and wind change and flooding probability on the Atlantic coast of France, *Oceanologica Acta*, *23*(6), 643-661.
Pugh, D. T. (1982), Estimating extreme currents by combining tidal and surge probabilities, *Ocean Engineering*, *9*(4), 361-372.
Sabatino, A. D., R. B. O’Hara Murray, A. Hills, D. C. Speirs, and M. R. Heath (2016), Modelling sea level surges in the Firth of Clyde, a fjordic embayment in south-west Scotland, *Natural Hazards*, *84*(3), 1601-1623.
Serafin, K. A., P. Ruggiero, and H. F. Stockdon (2017), The relative contribution of waves, tides, and non-tidal residuals to extreme total water levels on US West Coast sandy beaches, *Geophysical Research Letters*, *44*, 1839–1847.
Williams, J., K. J. Horsburgh, J. A. Williams, and R. N. F. Proctor (2016), Tide and skew surge independence: New insights for flood risk, *Geophysical Research Letters*, *43*(12), 6410-6417.

Wolf, J., and R. A. Flather (2005), Modelling waves and surges during the 1953 storm, *Philosophical Transactions of the Royal Society A: Mathematical, Physical and Engineering Sciences*, *363*(1831), 1359.
Wu, W., R. J. May, H. R. Maier, and G. C. Dandy (2013), A benchmarking approach for comparing data splitting methods for modeling water resources parameters using artificial neural networks, *Water Resources Research*, *49*(11), 7598-7614.
Yin, J., N. Lin, and D. Yu (2016), Coupled modeling of storm surge and coastal inundation: A case study in New York City during Hurricane Sandy, *Water Resources Research*, 52(11), 8685-8699.
Zheng, F., M. Leonard, and S. Westra (2015), Application of the design variable method to estimate coastal flood risk, Journal of Flood Risk Management.

Figure captions

Figure 1 Seasonal distribution of storm surge events (identified using the exponential basis function above selected threshold) and event peaks, illustrating: (a) the percentage of storm surge events in each of the seasons at each tide gauge; and (b) the percentage of storm surge events with peaks falling in each of the following ranges (from left to right): <0.4 m, 0.4 – 0.6 m, 0.6 – 0.8 m, 0.8 – 1.0 m, 1.0 – 1.2 m, 1.2 - 1.5 m and > 1.5 m. Maps were produced using the R package ggmap [*Kahle and Wickham*, 2013].

Figure 2 Hypothesis test results for (a) peak and (b) half-life of storm surge events simulated using the exponential basis function. The null hypothesis for each season is represented using box-and-whisker plots, for spring (green), summer (red), autumn (orange) and winter (blue). The upper and lower whiskers of the box plots indicate the 2.5th and 97.5th percentiles of the mean surge event peak obtained from bootstrap resampling; i.e. the 95% confidence interval. The brown asterisk indicates the observed mean value in each season.

Figure 3 Relationship between the peak and decay rate of storm surge events at three locations (Darwin, Hillarys and Lorne) in (a) summer and (b) winter, and associated evolution of storm surge events. The black cycles in figures in in the left column represent historical events; while the coloured circles represent fitted events, whose temporal evolution is illustrated in the corresponding figures in the right column. The relationship is statistically significant at $p<0.05$ at Darwin (north of Australia) in summer and at Hillarys and Lorne (south of Australia) in winter.

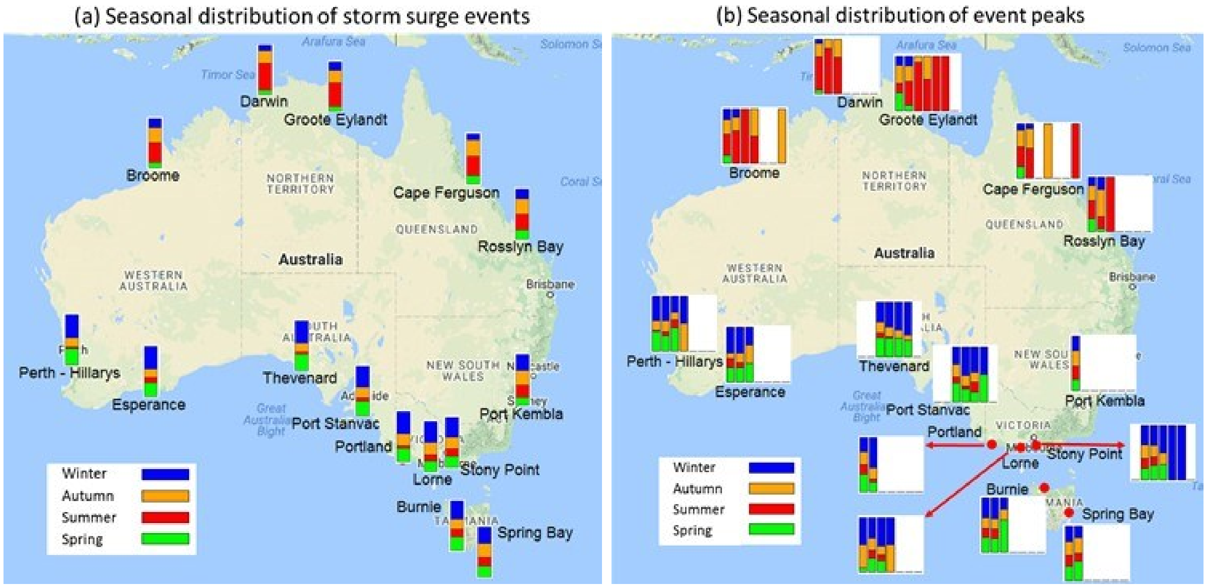
(a) Seasonal distribution of storm surge events
(b) Seasonal distribution of event peaks
Darwin
Groote Eylandt
Broome
Cape Ferguson
Rosslyn Bay
Australia
Perth - Hillarys
Esperance
Thevenard
Port Stanvac
Portland
Lorne
Stony Point
Port Kembla
Burnie
Spring Bay
Winter
Autumn
Summer
Spring

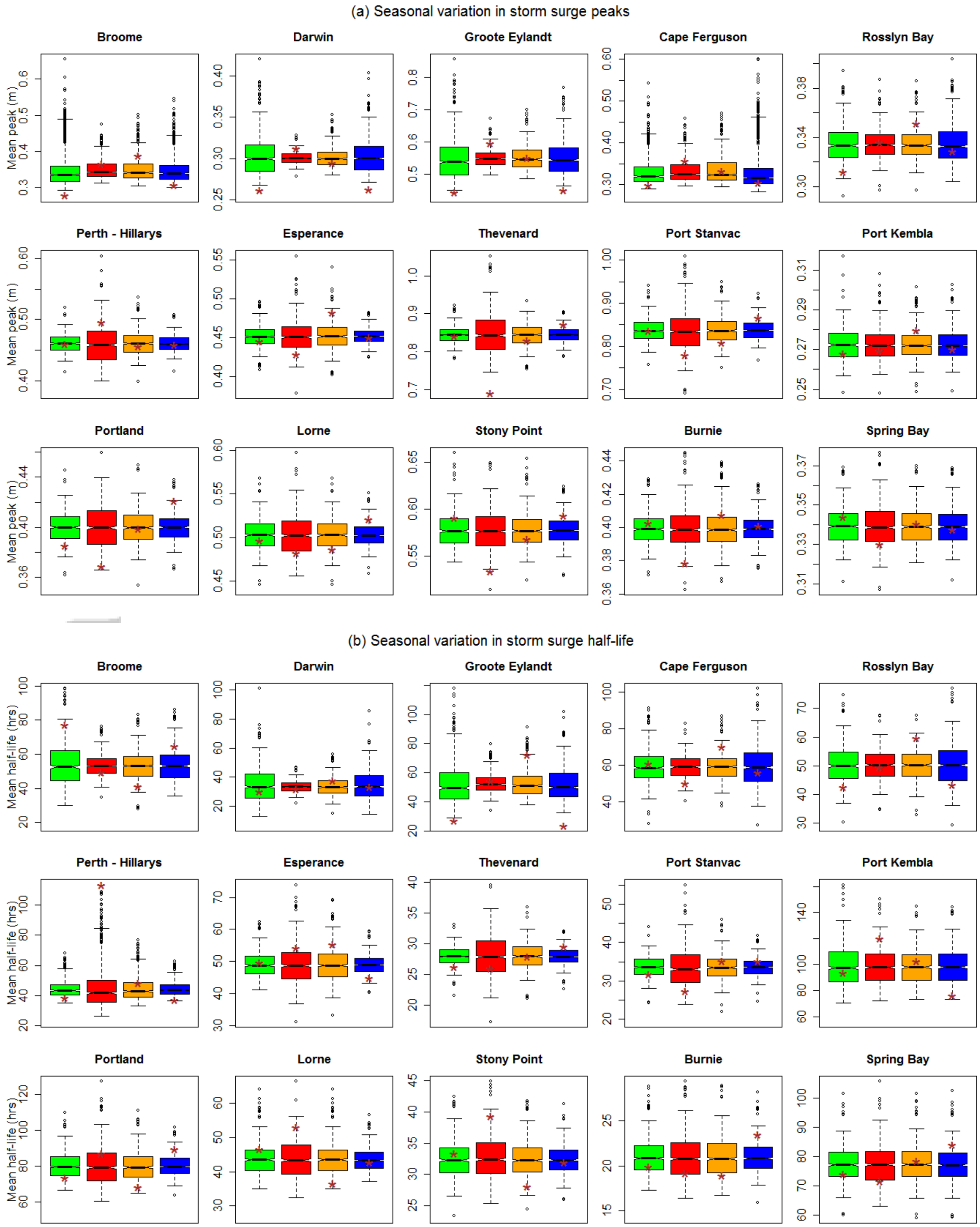
(a) Seasonal variation in storm surge peaks
Broome
Darwin
Groote Eylandt
Cape Ferguson
Rosslyn Bay
Perth - Hillarys
Esperance
Thevenard
Port Stanvac
Port Kembla
Portland
Lorne
Stony Point
Burnie
Spring Bay
Mean peak (m)
(b) Seasonal variation in storm surge half-life
Broome
Darwin
Groote Eylandt
Cape Ferguson
Rosslyn Bay
Perth - Hillarys
Esperance
Thevenard
Port Stanvac
Port Kembla
Portland
Lorne
Stony Point
Burnie
Spring Bay
Mean half-life (hrs)

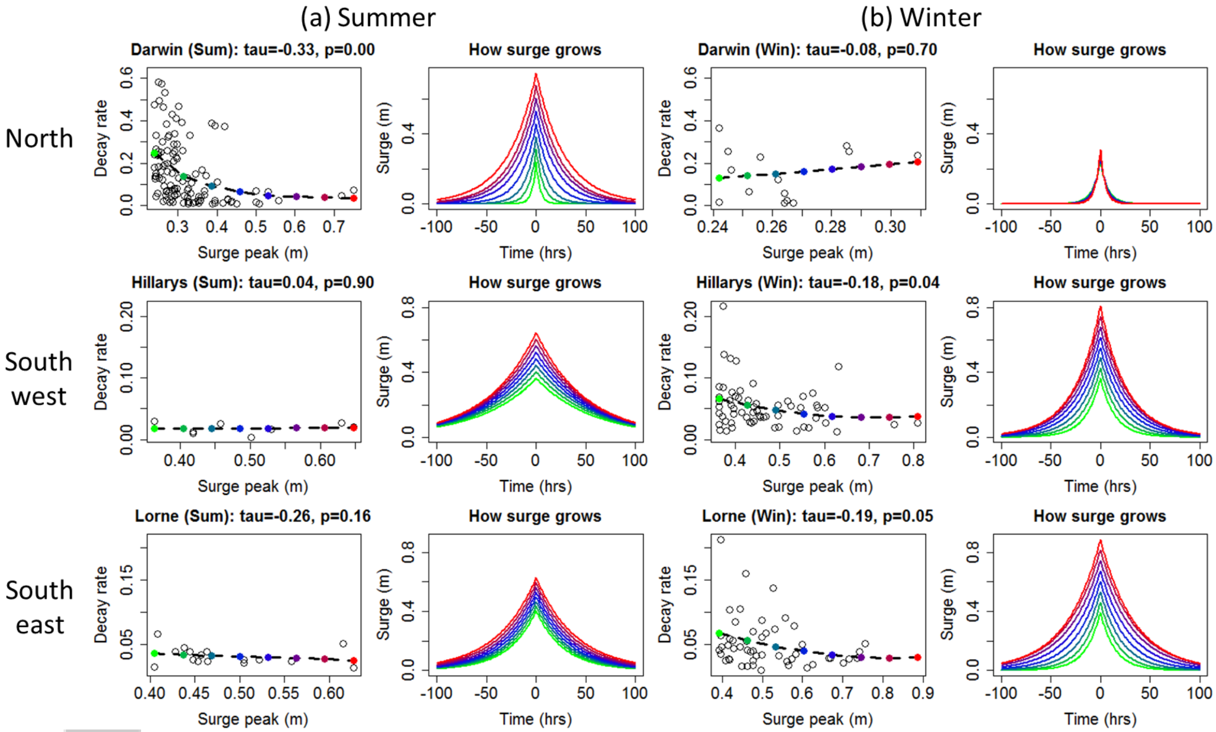
(a) Summer
(b) Winter
North
South west
South east
Darwin (Sum): tau=-0.33, p=0.00
Darwin (Win): tau=-0.08, p=0.70
Hillarys (Sum): tau=0.04, p=0.90
Hillarys (Win): tau=-0.18, p=0.04
Lorne (Sum): tau=-0.26, p=0.16
Lorne (Win): tau=-0.19, p=0.05
How surge grows
Decay rate
Surge peak (m)
Surge (m)
Time (hrs)